Food and Chemical Toxicology 127 (2019) 251–259

Contents lists available at ScienceDirect

Food and Chemical Toxicology

journal homepage: www.elsevier.com/locate/foodchemtox

Cyanidin chloride modestly protects Caco-2 cells from ZnO nanoparticle exposure probably through the induction of autophagy

Leying Jiang[a,b,1], Zhen Li[a,b,1], Yixi Xie[b], Liangliang Liu[a,**], Yi Cao[b,*]

[a] Institute of Bast Fiber Crops, Chinese Academy of Agricultural Sciences, Changsha, 410205, PR China
[b] Key Laboratory of Environment-Friendly Chemistry and Applications of Ministry Education, Laboratory of Biochemistry, College of Chemistry, Xiangtan University, Xiangtan, 411105, PR China

ARTICLE INFO

Keywords:
Cyanidin chloride (CC)
ZnO nanoparticle
Caco-2 cells
Cytotoxicity
Autophagy

ABSTRACT

Recent studies suggest that phytochemicals, as part of the food matrix, might alter the toxicity of nanoparticles (NPs); however, relatively few studies have investigated the impact of anthocyanidins on the toxicity of NPs to cells lining the gastrointestinal tract. Therefore, this study used cyanidin chloride (CC) as the model for anthocyanidins and investigated the effects of CC on the toxicity of ZnO or Ag NPs to Caco-2 cells. Exposure to ZnO but not Ag NPs significantly induced cytotoxicity. The presence of CC, but not its analog quercetin (Qu), modestly protected Caco-2 cells from ZnO NP exposure. However, the intracellular superoxide, Zn ions, or release of interleukin-8 after ZnO NP exposure were not significantly affected by the presence of CC. Rather, CC promoted the expression of autophagic genes *ATG5*, *ATG7*, and *BECN1* as well as the ratio of LC3-II/I after exposure to ZnO NPs. Meanwhile, the presence of autophagic inhibitors (chloroquine, NH_4Cl, bafilomycin A1) significantly promoted the cytotoxicity of ZnO NPs and inhibited the cytoprotective effects of CC. In conclusion, these data suggest that CC could modestly protect Caco-2 cells from ZnO NP exposure, probably through the induction of autophagy.

1. Introduction

The development of nanotechnologies increases the chances of oral exposure of humans to nanoparticles (NPs) in modern societies. Humans could be exposed to NPs orally when they digest food and food-related products (Wang et al., 2013), as NPs are increasingly added into products for many important applications, for instance nutrition improvement (Jain et al., 2018), anti-microorganisms (Wang et al., 2017b), and color development (Pathakoti et al., 2017). Moreover, oral exposure to NPs could also occur when used as healthcare materials, for example, NP-based formulations (Wang et al., 2017a; Yang et al., 2018) and dental materials (Feng et al., 2015). Indeed, oral, dermal, and inhalational exposure are the main routes for particles in daily life, but the potential toxic effects of NPs via oral exposure are significantly less studied compared with the other exposure routes (Vance et al., 2015). In addition, recent studies also highlight the importance of investigating the toxicity of NPs when present in food components due to their influence on the colloidal and toxicological aspects of NPs (Cao et al., 2016; McClements et al., 2017). This possibility has already been tested by studies using typical food components, such as saccharides (Chen et al., 2015; Go et al., 2018), free fatty acids (Fang et al., 2017; Jiang et al., 2016), and vitamin C (Wang et al., 2014).

The influence of phytochemicals as typical food components on the toxicity of NPs has only recently been studied. Phytochemicals are healthy components derived from plants, which may be added into food and food related products for their well-documented beneficial health effects, such as anti-inflammatory, anti-oxidative stress, and anti-cancer properties (Liao et al. 2016, 2018; Xiang et al., 2017). It has been shown that flavonols, such as quercetin and kaempferol, could partially reduce the toxicity of Ag NPs to Caco-2 cells by inhibiting Ag NP-induced oxidative stress (Martirosyan et al. 2014, 2016). In contrast, we recently found that 3-hydroxyflavone enhanced the cytotoxicity of ZnO NPs to Caco-2 cells because it promoted NP-cell interactions as well as NP-induced oxidative stress (Luo et al., 2018). The studies mentioned above suggest that phytochemicals might alter the toxicity of NPs through the modulation of oxidative stress. However, we also recently found that flavones or flavonols significantly inhibited the cytotoxicity

* Corresponding author.
** Corresponding author.
E-mail addresses: liuliangliang@caas.cn (L. Liu), caoyi39@126.com (Y. Cao).
[1] These two authors contributed equally to this work.

https://doi.org/10.1016/j.fct.2019.03.047
Received 18 December 2018; Received in revised form 23 February 2019; Accepted 24 March 2019
Available online 26 March 2019
0278-6915/

of ZnO NPs to Caco-2 cells, and was primarily related with the chemical structures rather than the anti-oxidative properties of polyphenols (Li et al., 2018; Zhang et al., 2018). This suggests that other signaling pathways rather than oxidative stress might determine the combined toxicity of NPs and phytochemicals.

Although previous studies have already investigated the influence of some types of phytochemicals on the toxicity of NPs, relatively few studies have investigated the interaction between anthocyanidins and NPs. Anthocyanins are pigments in vegetables and fruits which present well-documented beneficial health activities (Belwal et al., 2017; Khoo et al., 2017; Moosavi et al., 2018). Therefore, it is possible that humans could be orally co-exposed to anthocyanins and NPs. In this study, we used cyanidin chloride (CC) as a model for anthocyanidins and investigated the influence of CC on the toxicity of ZnO or Ag NPs to Caco-2 cells. CC was selected because cyanidin is a typical anthocyanidin widely present in food and food-related products in relatively large amounts (Ongkowijoyo et al., 2018). For comparison, we also studied the interactions between NPs and quercetin (Qu), the chemical analog of CC (Supplemental Fig. S1), in order to assess the possible influence of polyphenol chemical structure in defining the interactions (Cao et al., 2017). ZnO and Ag NPs were used in this study, since they are among the most popular inorganic NPs used in food and food related products (Jain et al., 2018; Wang et al., 2013). More specifically, ZnO and Ag NPs could be used as alternatives to antibiotics due to their well-documented antibacterial activity (Gaillet and Rouanet, 2015; Krol et al., 2017). Besides, ZnO NPs could also be used as food additives for Zn supplement (Wang et al., 2013). The study design is illustrated in Supplemental Fig. S2. To indicate the influences of CC or Qu on colloidal properties of NPs, the changes of hydrodynamic size and zeta potential were measured. In addition, the total soluble Zn was also determined to indicate the influence of CC on solubility of ZnO NPs. We measured these endpoints because it has been suggested that food components could alter the colloidal properties of NPs leading to changes of NP-induced biological responses (Cao et al., 2016; McClements et al., 2017). The effects of CC or Qu on NP-induced cytotoxicity were studied in Caco-2 cells. Because we observed a cytoprotective effect of CC against ZnO NP exposure, we then measured oxidative stress, accumulation of intracellular Zn ions, release of inflammatory markers, since these endpoints are generally considered to correlate with the toxicity of ZnO NPs (Liu et al., 2016; Saptarshi et al., 2015). Moreover, previous studies showed that phytochemicals Qu partially reduced the cytotoxicity of Ag NPs to Caco-2 cells by inhibiting oxidative stress and/or inflammatory responses (Martirosyan et al. 2014, 2016). In contrast, food component vitamin C markedly enhanced the toxicity of ZnO NPs by promoting the accumulation of intracellular Zn ions (Wang et al., 2014). Thus, food components might change the toxicity of NPs to Caco-2 cells by influencing these endpoints. Surprisingly, we found that these endpoints were not significantly affected by the presence of CC. For this reason, we measured autophagy signaling pathways to explore the possible mechanisms. Autophagy is a tightly-regulated catabolic pathway that can degrade damaged organelles and macromolecules. Therefore, induction of autophagy pathway by exposure to environmental chemicals can promote the survival of cells under stressed conditions, although prolonged autophagy induction could also lead to cell death termed as autophagic cell death (Anozie and Dalhaimer, 2017; Pesonen and Vahakangas, 2019). Interestingly, nutrients (Hotamisligil, 2017; Hotamisligil and Erbay, 2008), including phytochemicals (Choe et al., 2012; Li et al., 2017), have been shown to modulate autophagy to generate beneficial/adverse health effects. However, the effects of co-exposure to NPs and phytochemicals on autophagy signaling pathways, to the best of our knowledge, have not been studied before.

2. Materials and methods

2.1. Cell culture

Caco-2 cells (ATCC, HTB-37), used as the model for human intestinal cells, were cultured in supplemented Dulbecco's Modified Eagle Medium (DMEM)/high glucose (Hyclone, GE Healthcare) and used within 5 cell passages as we have described previously (Li et al., 2018).

2.2. Particle characterization and preparation

Nanoparticles of ZnO (code XFI06; 20 nm) and Ag (code XFJ14; 80–90 nm) were obtained from Nanjing XFNANO Materials Tech Co., Ltd (Nanjing, China). The supplier information regarding the physicochemical properties of these NPs is summarized in Supplemental Table S1. In this study, the morphology and topography of these NPs were further investigated by transmission electron microscopy (TEM). In short, ZnO or Ag NPs were briefly sonicated in EtOH, and then a drop of suspension was deposited and dried on a carbon-coated grid. The samples were coated with a conductive layer of Au, and then the images were taken by a TEM accelerated at 200 kV (FEI Tecnai G20, USA). The size was calculated based on the quantification of 50 randomly selected particles measured by ImageJ (National Institutes of Health).

To make the suspension of ZnO or Ag NPs, 1 mg/mL of particles were suspended in Milli-Q water and then sonicated continuously for 8 min each on ice twice using an ultrasonic processor FS-250N (20% amplitude; Shanghai Shengxi, China). After sonication, the particles were diluted in cell culture medium to the desired concentrations for exposure. To indicate the changes in the colloidal properties of NPs due to the presence of CC or Qu (Shanghai Yuanye Biotechnology Co., Ltd., Shanghai, China), the hydrodynamic size and zeta potential distribution of 25 μg/mL XFI06 suspended in Milli-Q water with or without the presence of 50 μM CC or Qu was measured by Zetasizer nano ZS90 (Malvern, UK).

2.3. Zn trace element measurement

The concentrations of total soluble Zn released from the dissolution of XFI06 in different suspensions were measured using an atomic absorption spectrometer (AAS). Briefly, a total of 25 μg/mL XFI06 was suspended in water or cell culture medium with or without the presence of 50 μM CC. The suspensions were aged for 24 h at 37 °C in a CO_2 incubator, and then centrifuged at 16 000 × *g* for 30 min to separate NPs and soluble Zn. The concentrations of Zn trace element in supernatants were measured by an AA7000 AAS (Shimadzu CO., LTD, Japan) as previously described (Gong et al., 2017b). The experiment was conducted once (n = 4).

2.4. Cytotoxicity assays

The cytotoxicity was assessed by two independent assays, namely the cell counting kit-8 (CCK-8) and neutral red uptake assays, using commercial kits and following the manufacturer's instructions (Beyotime, Nantong, China). Briefly, 6×10^4 Caco-2 cells per well were seeded in 24-well plates and grown for 48 h before exposure. The cells were then incubated with 0 (control), 5, 10, 25, 50, or 100 μg/mL XFI06 or XFJ14, with or without the presence of 50 μM CC or Qu, for 24 h. The concentrations used in this study were comparable to those used in previous nanotoxicological studies with similar purpose (McCracken et al., 2016), although in real life, the exposure concentrations of ZnO NPs to human intestinal cells may be lower (Moreno-Olivas et al., 2019). After exposure, the cells were rinsed once followed by CCK-8 and neutral red uptake assays according to manufacturer's instructions. The products were read by a microplate reader (Synergy HT, BioTek, Woburn, MA, USA).

To explore the possible role of autophagy in the toxicity of ZnO NPs,

Caco-2 cells were exposed to 25 μg/mL XFI06 or 25 μg/mL XFI06 plus 50 μM CC with or without the presence of autophagic inhibitors, including 50 μM chloroquine (CQ; Sigma-Aldrich, Saint Lois, MO, USA), 10 mM NH_4Cl (Aladdin Chemistry, Shanghai, China) or 100 nM bafilomycin A1 (Baf A1; CST Cell Signaling Technologies, USA). CQ impairs lysosomal function as it can accumulate in lysosomes in protonated form to increase lysosomal pH (Kimura et al., 2013). NH_4Cl is a lysosomal protease inhibitor that can inhibit autophagic flux (Xia et al., 2016). Baf A1 blocks autophagic flux by inhibiting vacuolar H^+ ATPase activity leading to impaired fusion between autophagosomes and lysosomes (Wang et al., 2019). All of these inhibitors arrest late phase of autophagy via different mechanisms. After 24 h exposure, the cytotoxicity was measured by CCK-8 assay as indicated.

2.5. Intracellular superoxide

The intracellular superoxide was measured by a dihydroethidium fluorescent probe (DHE; Beyotime, China). Briefly, 1.5×10^4 per well of Caco-2 cells were grown on 96-well black plates for 2 days. Then, the cells were exposed to high levels of XFI06 (0, 5, 10, 25, 50, or 100 μg/mL) for a short term (3 h) or low levels of XFI06 (0, 5, 10, or 20 μg/mL, lower than EC50) for a long term (24 h), with or without the presence of 50 μM CC. After that, the cells were rinsed once with Hanks' solution, incubated with 10 μg/mL DHE (Beyotime, Nantong, China) for 30 min in the dark, and then rinsed with Hanks' solution. The red fluorescence was read at Ex 530 ± 25 nm and Em 590 ± 35 nm by a microplate reader.

2.6. Intracellular Zn ions

Caco-2 cells were exposed to XFI06 with or without the presence of CC as described in DHE measurement, and the accumulation of intracellular Zn ions was measured using a Zinquin ethyl ester fluorescent probe (Sigma-Aldrich, USA) as previously described (Jiang et al., 2016).

2.7. ELISA

Caco-2 cells were exposed to 0 (control), 5, 10, or 20 μg/mL XFI06 with or without the presence of 50 μM CC for 24 h, and the supernatants were collected for ELISA analysis. The release of interleukin 8 (IL-8) was determined by an ELISA kit according to manufacturer's instructions (Neobioscience Technology Co., Ltd., Guangzhou, China). The detection limit is 3.9 pg/mL, and the concentrations of IL-8 in all the samples were higher than the detection limit. We measured IL-8 because it is a biomarker for inflammatory responses, and previously it has been shown that phytochemicals prevented the release of IL-8 from Ag NP-exposed Caco-2 cells (Martirosyan et al. 2014, 2016). Moreover, we previously found that Caco-2 cells released IL-8 in relatively large amount, whereas the concentrations of other cytokines, such as IL-1β and IL-6, were low or even undetectable by conventional ELISA analysis (Gong et al., 2017b; Li et al., 2018). The concentrations of ZnO NPs used to expose cells are below EC50, so it is expected that most of the cells are viable during the exposure period to release IL-8.

2.8. Real time RT-PCR

The mRNA level of autophagic genes (*ATG5*, *ATG7*, and *BECN1*) were determined by quantitative real time RT-PCR, using *GAPDH* as internal control. Briefly, 3×10^5 Caco-2 cells per well were seeded on 6-well plates and grown for 2 days before exposure to 0 (control) or 25 μg/mL XFI06 or 25 μg/mL XFI06 plus 50 μM CC for 24 h. After exposure, the total mRNA was extracted by TRI Reagent® following manufacturer's instructions (Sigma-Aldrich, USA), and the quantitative real-time PCR was conducted using UltraSYBR Mixture (CW biotech, Beijing, China) on a PikoReal™ qPCR system (Thermo-Fisher, USA). The primers for each gene are summarized in Supplemental Table S2.

2.9. Western blot

Caco-2 cells were exposed to 0 μg/mL (control), 25 μg/mL XFI06 or 25 μg/mL XFI06 plus 50 μM CC for 24 h as indicated above, and the protein levels of LC3-I and LC3-II were determined by Western blot. Briefly, after rinsed rinsed twice with Hank's solution, the proteins from each sample were extracted using radioimmunoprecipitation assay lysis buffer, protease inhibitor cocktail and PhosStop™ phosphatase inhibitor (Roche Diagnostics). After placed on ice for 10 min and centrifugation, the protein concentrations in the supernatants were measured with bicinchoninic acid method. For each sample, a total of 50 μg protein was mixed with a loading buffer and resolved by sodium dodecyl sulfate polyacrylamide gel electrophoresis. The samples were transferred onto a nitrocellulose membrane, blocked with non-fat milk for 1.5 h at room temperature, and incubated overnight at 4 °C with primary antibody (1:1000 LC3, CST Cell Signaling Technologies, USA; 1:5000 β-actin antibody, Proteintech, USA). The blots were washed with 0.1% w/v Tween-PBS and incubated with 1:5000 horseradish peroxidase goat anti-rabbit IgG (Proteintech, USA) for 1.5 h. The blots were detected with SuperECL Plus chemiluminescence (Thermo pierce, USA). The density of the band was determined by using ImageJ (National Institutes of Health).

2.10. Statistics

All the data are expressed as means ± standard deviation (SD) of 3–4 independent experiments. Two-way ANOVA was conducted to measure the interactions between NPs and CC/Qu, followed by Tukey HSD test to compare the difference using R 3.2.2. The p value < 0.05 was considered as statistically different.

3. Results

3.1. Characteristics of NPs

According to the information provided by the supplier, XFI06 and XFJ14 are pristine ZnO and Ag NPs without any surface coatings (summarized in Supplemental Table S1). The representative TEM images of these NPs are shown in Fig. 1. Both NPs contain spherical and irregular particles. The primary sizes of XFJ14 and XFI06 were calculated as 67.4 ± 27.5 nm (size range 25–150 nm) and 34.1 ± 9.5 nm (size range 15–55 nm), respectively.

3.2. Changes in colloidal properties of NPs

The representative images of hydrodynamic size and zeta potential distribution of XFI06 and XFJ14 with or without the presence of CC or Qu are shown in Supplemental Fig. S3 and S4, respectively. Table 1 summarizes the changes in hydrodynamic size and zeta potential of NPs due to the presence of CC or Qu. Without the presence of CC or Qu, both NPs had hydrodynamic size much larger than their TEM size, which indicated the presence of agglomerates and/or aggregates of particles in suspension. An increase in hydrodynamic size was only observed when XFI06 was incubated with CC but not Qu. Both NPs had negative zeta potential. The presence of Qu decreased zeta potential of XFI06 but increased that of XFJ14, whereas CC did not influence the zeta potential of XFI06 or XFJ14.

The total soluble Zn concentrations were measured by AAS to indicate the solubility of XFI06 in different suspensions (shown in Supplemental Fig. S5). The presence of CC had minimal impact on the solubility of XFI06, although the concentrations of total soluble Zn were slightly increased when XFI06 was incubated with CC in cell culture medium.

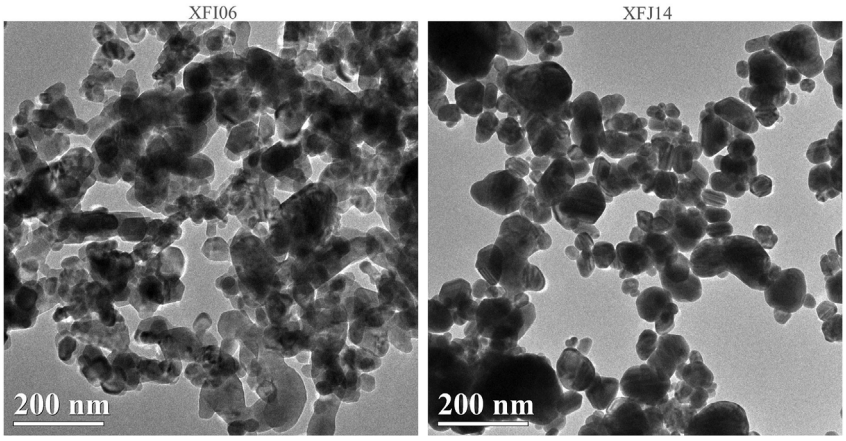

Fig. 1. The morphology of XFI06 (ZnO nanoparticles; left column) and XFJ14 (Ag nanoparticles; right column) by transmission electron microscopy.

3.3. Cytotoxicity

The dose-dependent cytotoxicity curves of XFI06 with or without the presence of CC or Qu are shown in Fig. 2. For both CCK-8 (Fig. 2A) and neutral red uptake assays (Fig. 2B), the presence of CC slightly reduced the cytotoxicity of XFI06, and EC50 value was increased from 22.49 μg/mL to 26.66 μg/mL (determined by CCK-8 assay) or 23.33 μg/mL to 25.26 μg/mL (determined by neutral red uptake assay) due to the presence of CC. In contrast, the presence of Qu did not obviously affect the cytotoxicity, and EC50 values were 18.62 μg/mL (determined by CCK-8 assay) or 22.10 μg/mL (determined by neutral red uptake assay) when Qu was present.

The cytotoxicity of XFJ14 to Caco-2 cells with or without the presence of CC or Qu is shown in Supplemental Fig. S6. Exposure to various concentrations of XFJ14 did not significantly induce cytotoxicity ($p > 0.05$), and the presence of CC or Qu did not affect the toxicity of XFJ14 ($p > 0.05$).

3.4. Intracellular superoxide

The measured intracellular superoxide is shown in Fig. 3. It was shown that the intracellular superoxide was not significantly affected after 3 h (Fig. 3A) or 24 h (Fig. 3B) exposure to various concentrations of XFI06, with or without the presence of CC ($p > 0.05$).

3.5. Intracellular Zn ion concentration after ZnO NP exposure

Exposure to various concentrations of XFI06 for 3 h (Fig. 4A) or 24 h (Fig. 4B) significantly increased the intracellular Zn ions ($p < 0.01$ for all concentrations), although the increase of intracellular Zn ions appeared to be more modest after 3 h exposure (Fig. 4A). The increase of intracellular Zn ions following XFI06 exposure was not significantly influenced by the presence of CC ($p > 0.05$).

3.6. Release of IL-8 after ZnO NP exposure

The release of IL-8 was determined by ELISA and shown in Supplemental Fig. S7. Exposure to XFI06 at concentrations lower than EC50 (up to 20 μg/mL), with or without the presence of CC, did not significantly affect the release of IL-8 ($p > 0.05$).

3.7. Change in autophagic biomarkers following exposure to NPs

Fig. 5 shows the changes of expression in autophagic genes and proteins following NP exposure. As shown in Fig. 5A, the expression of *ATG5* was significantly down-regulated by XFI06 alone ($p < 0.05$) but up-regulated by XFI06 plus CC ($p < 0.05$). For *ATG7* (Fig. 5B), its expression was only modestly increased after exposure to XFI06 ($p > 0.05$) but significantly increased after exposure to XFI06 plus CC ($p < 0.01$). For *BECN1* (Fig. 5C), its expression was only significantly promoted by XFI06 plus CC ($p < 0.01$). The expression of *ATG5*, *ATG7*, and *BECN1*, following exposure to XFI06 plus CC, induced a significantly higher expression of these genes compared with that of XFI06 alone ($p < 0.01$). For protein levels of LC3-I and LC3-II (Fig. 5D), exposure to XFI06 decreased LC3-II/LC3-I ratio, which was partially reversed by CC.

3.8. The influence of autophagic inhibitors on the cytotoxicity

As shown in Fig. 6, the presence of different types of autophagic inhibitors, namely CQ, NH_4Cl, and Baf A1, all significantly decreased the cellular viability after XFI06 exposure ($p < 0.01$ for all). The presence of CC modestly promoted the cellular viability of Caco-2 after XFI06 challenge by about 30% ($p < 0.01$), which was significantly inhibited by the presence of CQ, NH_4Cl ($p < 0.01$), and Baf A1 ($p < 0.05$). However, the effects of Baf A1 appeared to be less effective, with the cellular viability after XFI06 plus CC and Baf A1 exposure still significantly higher than that after XFI06 exposure ($p < 0.05$), whereas the presence of CQ and NH_4Cl completely abolished the cytoprotective effects of CC against XFI06 exposure.

4. Discussion

This study investigated the interactions between ZnO/Ag NPs and a typical anthocyanidin, CC. Previous studies have shown that CC could change the colloidal stability of NPs; however, these effects appeared to be minimal in our study. Exposure to ZnO, but not Ag NPs, was associated with cytotoxicity, whereas CC modestly protected Caco-2 cells

Table 1
The hydrodynamic size and Zeta potential of ZnO NPs (Code: XFI06) and Ag NPs (Code: XFJ14) in different suspensions.

	XFI06	XFI06 + CC	XFI06 + Qu	XFJ14	XFJ14 + CC	XFJ14 + Qu
Size (nm)	272.5 ± 1.3	341.3 ± 10.7	278.6 ± 3.1	112.2 ± 1.7	115.2 ± 1.8	113.9 ± 2.8
Zeta potential (mV)	−17.0 ± 0.5	−17.6 ± 0.5	−21.5 ± 0.2	−18.8 ± 0.5	−18.8 ± 0.2	−13.5 ± 0.7

Data were expressed as mean ± SD of three measurement based on a single run.

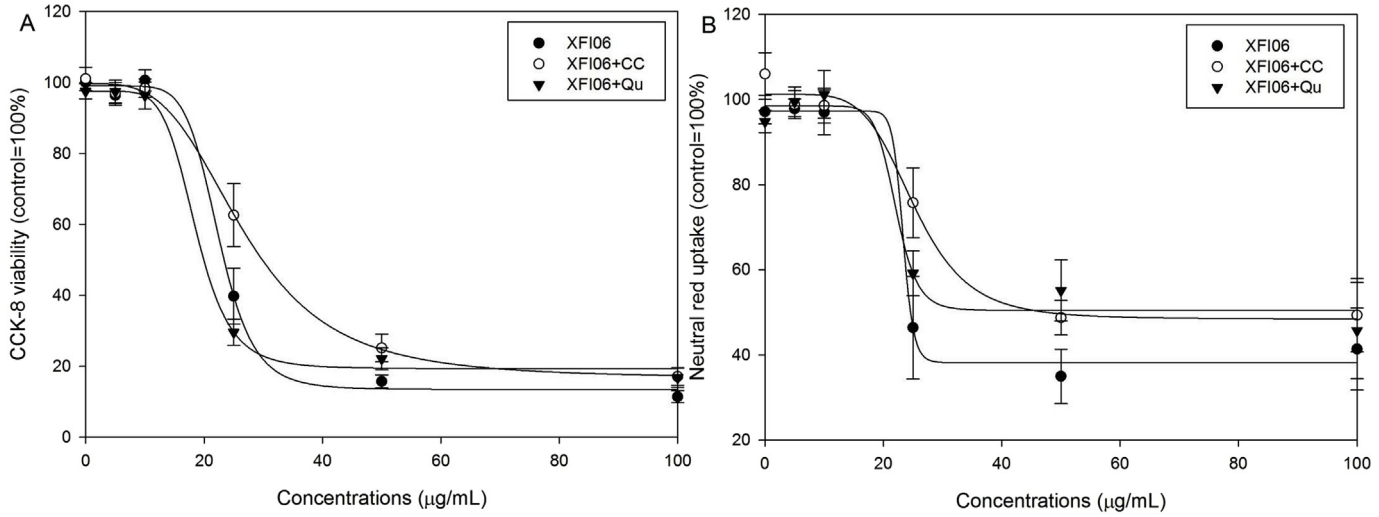

Fig. 2. Cytotoxicity of XFI06 (ZnO NPs) to Caco-2 cells as assessed by cell counting kit 8 (CCK-8) (2A) and neutral red uptake assays (2B). Caco-2 cells were exposed to various concentrations of XFI06 with or without the presence of 50 μM CC or Qu for 24 h, and CCK-8 and neutral red uptake assays were used to indicate the cytotoxicity. Data were expressed as mean ± SD of four independent experiments (n = 3 for each). The lines indicate the dose–response curve of the four-parameter logistic equation, and the EC50 was calculated.

from ZnO NP exposure. For comparison, Qu, the chemical analog of CC, did not exhibit this effect. ZnO NPs did not significantly influence intracellular superoxide or release of IL-8 but significantly promoted intracellular Zn ions, which was not significantly affected by CC. However, the expression of autophagic genes, namely *ATG5*, *ATG7*, and *BECN1*, as well as the ratio of LC3-II/LC3-I, increased after co-exposure to CC and ZnO NPs compared with exposure to ZnO NPs alone. Furthermore, the presence of autophagic inhibitors significantly enhanced the cytotoxicity of ZnO NPs and could inhibit the cytoprotective effects of CC, suggesting a role for autophagy. To the best of our knowledge, this is the first study to investigate the interactions between NPs and anthocyanidins.

Previous studies have shown that typical food components, such as sugar, vitamin C, and free fatty acids, could change the colloidal stability of NPs (Chen et al., 2015; Go et al. 2017, 2018; Lee et al., 2017; Wang et al., 2014). In the case of phytochemicals, we have also recently shown that flavones or flavonols could influence the colloidal properties such as hydrodynamic size, zeta potential, and solubility of ZnO NPs (Li et al., 2018; Zhang et al., 2018). Consistent with previous reports, our data also demonstrated that CC or Qu might influence the same colloidal properties of ZnO NPs (Table 1 and Supplemental Fig. S2–S4). However, compared with our recent studies focusing on other phytochemicals (Li et al., 2018; Luo et al., 2018; Zhang et al., 2018), the influence of CC on the colloidal properties of ZnO NPs appeared to be minimal and is probably not responsible for the changes of cytotoxicity of NPs. Nevertheless, when assessing the combined toxicological effects of NPs and phytochemicals, it is still necessary to measure the influence of phytochemicals on the colloidal stability of NPs, as the inclusion of food components might alter the NP-gastrointestinal cell interactions with the NPs (McClements et al., 2017; Moore et al., 2015).

We then investigated the changes in cytotoxicity of NPs due to the presence of phytochemicals by determining the changes of EC50. ZnO but not Ag NPs significantly induced cytotoxicity to Caco-2 cells, whereas CC but not Qu protected Caco-2 cells from ZnO NP exposure (Fig. 2). In our preliminary experiment, we found that Ag colloidals (code XFJ13, size 15 nm) and Ag nanoflake (code XFJ45, size 5 μm) at concentrations up to 100 μg/mL were not cytotoxic to Caco-2 cells (data not shown). Therefore, we suggest that uncoated Ag NPs up to 100 μg/mL are not cytotoxic to our model used in this study. This is also consistent with previous studies showing that ZnO NPs were significantly

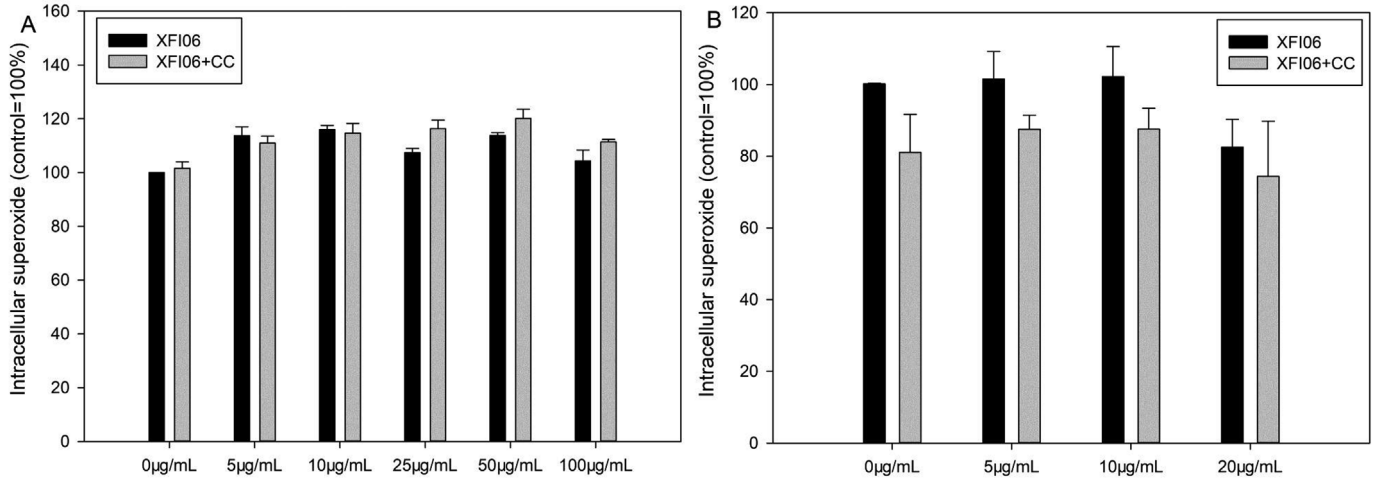

Fig. 3. The intracellular superoxide in XFI06 (ZnO NPs) exposed Caco-2 cells. Caco-2 cells were exposed to 100 μg/mL to 5 μg/mL XFI06 for 3 h (3A) or 20 μg/mL to 5 μg/mL XFI06 (3B) for 24 h with or without the presence of 50 μM CC. After exposure, the intracellular superoxide was determined by a fluorescent probe. Data were expressed as mean ± SD of three independent experiments (n = 3 for each).

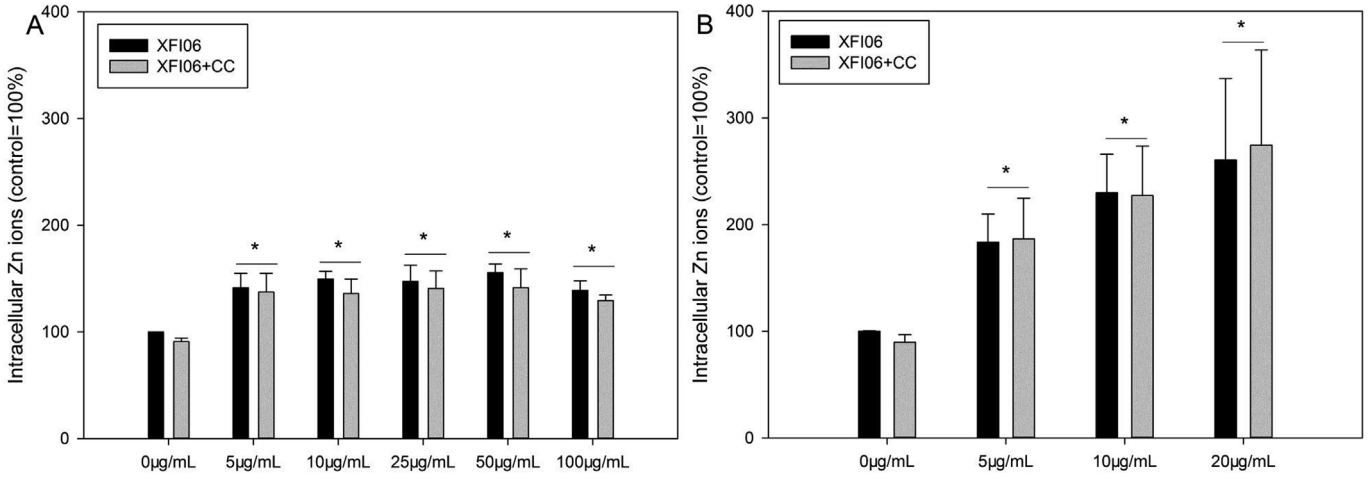

Fig. 4. The intracellular Zn ions in XFI06 (ZnO NPs) exposed Caco-2 cells. Caco-2 cells were co-exposed to 100 μg/mL to 5 μg/mL XFI06 for 3 h (4A) or 20 μg/mL to 5 μg/mL XFI06 (4B) for 24 h with or without the presence of 50 μM CC. After exposure, the intracellular Zn ions were determined by a fluorescent probe. Data were expressed as mean ± SD of four independent experiments (n = 3 for each). *, $p < 0.01$, compared with that of the control.

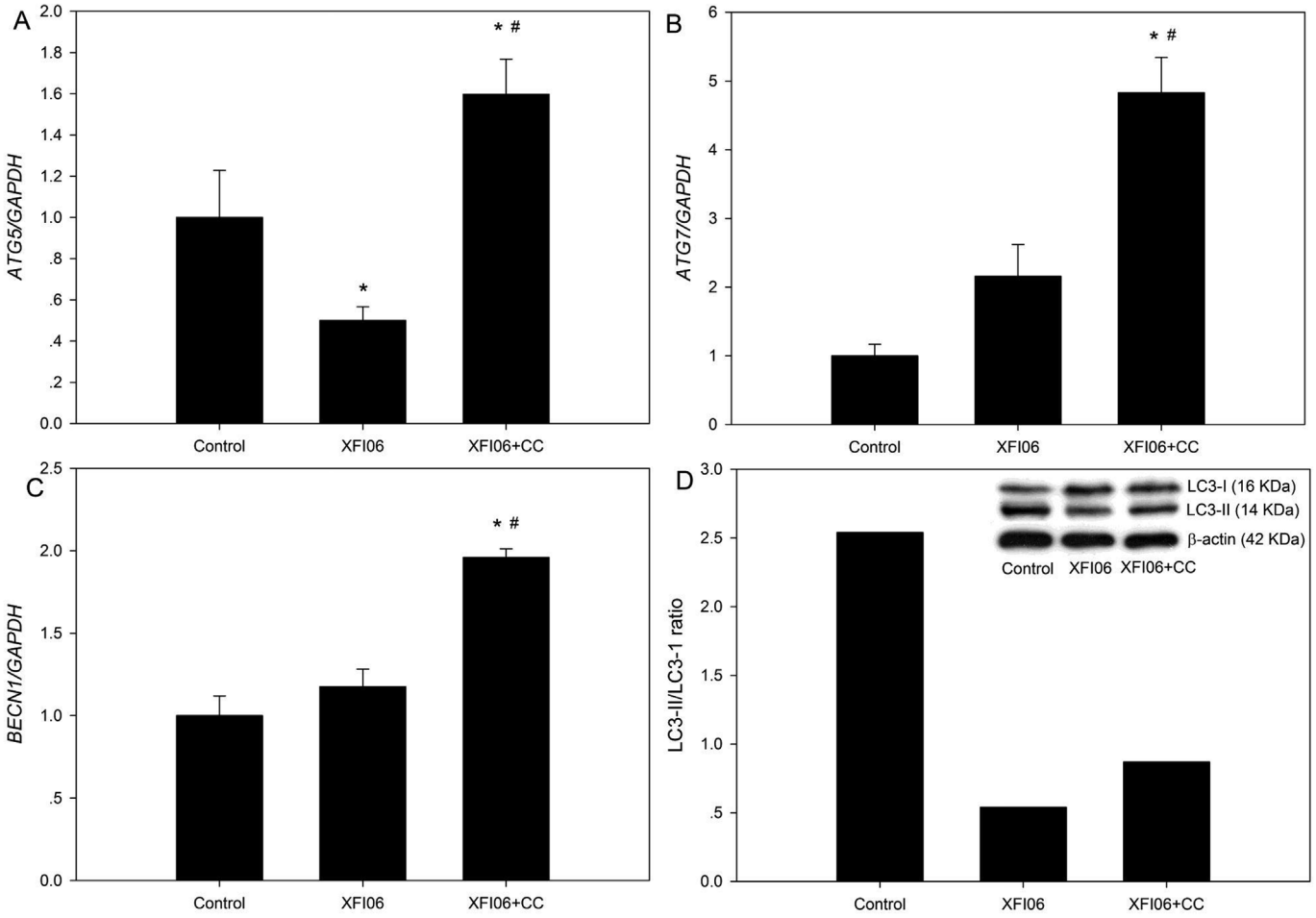

Fig. 5. The autophagic signaling pathway of XFI06 (ZnO NPs) exposed Caco-2 cells. Caco-2 cells were exposed to 25 μg/mL XFI06 with or without the presence of 50 μM CC for 24 h. After exposure, the expression of *ATG5* (5A), *ATG7* (5B), and *BECN1* (5C) was measured by real time RT-PCR, and the protein levels of LC3-I and LC3-II were determined by Western blot (5D). For RT-PCR data, they were expressed as mean ± SD of three independent experiments (n = 3 for each). *, $p < 0.05$, compared with control; #, $p < 0.01$, compared with the cells exposed to XFI06 alone.

more cytotoxic to Caco-2 cells compared with uncoated Ag NPs based on the same mass concentrations (Abbott Chalew and Schwab, 2013; Mao et al., 2016; Song et al., 2014). The cytoprotective effects of only CC indicates a possible role of the chemical structure of the phytochemicals in defining the toxicity of NPs, in agreement with our recent report (Zhang et al., 2018). To the best of our knowledge, no previous studies have investigated the combined toxicity of CC and NPs; however, a recent study did show that cyanidin reduced the toxicity of

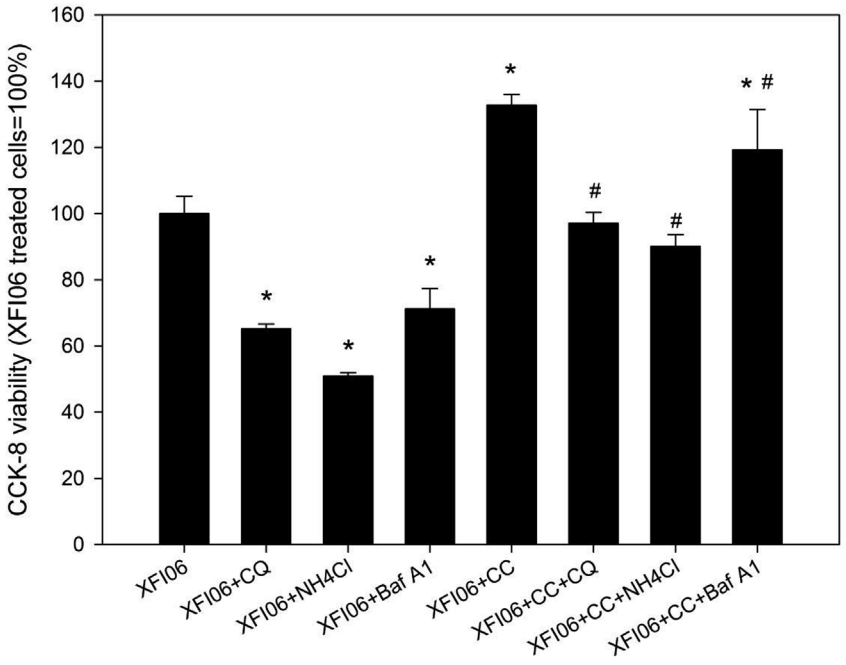

Fig. 6. The influence of autophagic inhibitors on the cytotoxicity of XFI06 (ZnO NPs). Caco-2 cells were exposed to 25 μg/mL XFI06 or 25 μg/mL XFI06 plus 50 μM CC with or without the presence of 50 μM chloroquine (CQ), 10 mM NH_4Cl or 100 nM bafilomycin A1 (Baf A1). After 24 h exposure, the cytotoxicity was measured by cell counting kit 8 assay. Data were expressed as mean ± SD of three independent experiments (n = 3 for each). *, $p < 0.05$, compared with control; #, $p < 0.05$, compared with the cells exposed to XFI06 alone.

cisplatin to cardiomyocytes (Qian et al., 2018). In another study, it was shown that cyanidin-3-O-glucoside protected rat Leydig cells from lead exposure (Wen et al., 2018). Thus, it is possible that CC could reduce the toxicity of metals, although more studies examining different types of metal-based NPs are needed to confirm it.

Previous studies suggest that phytochemicals protect Caco-2 cells from the toxicity of Ag NPs due to the anti-oxidative and anti-inflammatory properties of the phytochemicals (Martirosyan et al. 2014, 2016). Here, the results from this study showed unaltered intracellular superoxide (Fig. 3) or release of IL-8 (Supplemental Fig. S6) after ZnO NP exposure with or without the presence of CC. These results are consistent with our previous studies showing that ZnO NP exposure did not induce oxidative stress or inflammatory responses in Caco-2 cells (Fang et al., 2017; Gong et al., 2017b; Li et al., 2018). Rather, excessive intracellular Zn ion concentrations were induced after ZnO NP exposure (Fig. 4), which could be responsible for the cytotoxicity of ZnO NPs (Liu et al., 2016; Saptarshi et al., 2015). However, although CC protected Caco-2 cells from ZnO NP exposure, it did not significantly affect the concentration of intracellular Zn ions, indicating that CC might not change the internalization of NPs. This might be due to CC having minimal impact on the colloidal properties of ZnO NPs, as discussed above. In our previous studies, we found that saturated fatty acids did not significantly affect the intracellular Zn ions but enhanced the cytotoxicity of ZnO NPs (Gong et al., 2017a; Jiang et al., 2016), which we suggested was probably due to the intrinsic toxicity of fatty acids (Gong et al., 2017b). Therefore, CC might also influence the toxicity of ZnO NPs due to other mechanisms than direct changes in NP-cell interactions.

To explore the possible mechanisms associated with the observed cytoprotective effects of CC against ZnO NP exposure, we investigated the autophagic pathway. Here we observed decreased expression of *ATG5* (Fig. 5A) and conversion of LC3-I to LC3-II (Fig. 5D) after ZnO NP exposure. The decreased expression of typical autophagic genes following ZnO NP exposure was recently reported by us, which could be related with the cytotoxicity of ZnO NPs to lung epithelial cells (Liu et al., 2019). Interestingly, co-exposure to ZnO NPs and CC led to significantly higher expression of *ATG5*, *ATG7*, *BECN1*, and partially increased LC3-II/LC3-I ratio compared with the exposure to ZnO NPs alone (Fig. 5). It has been suggested that autophagy and caspase-mediated apoptosis are cross-regulated (Tsapras and Nezis, 2017). However, in our preliminary experiment the mRNA levels of pro-apoptotic regulators, such as *BAX*, *CASP3* and *CASP7*, were not significantly down-regulated after co-exposure to ZnO NPs and CC compared with exposure of ZnO NPs alone (data not shown). Therefore, we suggest that CC could increase autophagic activities following ZnO NP challenge without an effect on apoptotic pathways. Previously, extensive studies showed that NPs induced prolonged activation of autophagy as the mechanisms for cell death, but few studies showed the induction of autophagy as an essential protective mechanism against particle challenge. For instance, it has been shown before that Ag NPs (Lin et al. 2014, 2018), quantum dot (Luo et al., 2013), and CuO NPs (Laha et al., 2014), induced a cytoprotective autophagy, that inhibition of autophagic activities promoted the cytotoxicity of NPs. This is consistent with our results here showing that autophagic inhibitors significantly enhanced the cytotoxicity of ZnO NPs and abolished the protective effects of CC (Fig. 6). Therefore, we suggest that the induction of autophagic genes and proteins by CC is also cytoprotective, which promotes the survival of Caco-2 cells in response to ZnO NP exposure. This is also consistent with previous studies showing that CC could generate health benefits and promote the survival of cells through the modulation of autophagy (Choe et al., 2012; Li et al., 2017).

In combination, the results from this study showed that CC and Qu could influence the colloidal aspects of ZnO and Ag NPs, but the effects were minimal. Exposure to ZnO, but not Ag, NPs significantly induced cytotoxicity, and the presence of CC modestly protected Caco-2 cells from ZnO NP exposure. The cytotoxicity of ZnO NPs to Caco-2 cells was associated with increased intracellular Zn ions but not superoxide or release of IL-8, whereas these endpoints were not significantly affected by CC. However, co-exposure to CC and ZnO NPs led to higher expression of typical autophagic genes and the ratio of LC3-II/LC3-I, and the presence of autophagic inhibitors inhibited the cytoprotective effects of CC against ZnO NP exposure, which suggests that CC might protect Caco-2 cells from ZnO NP exposure probably through the induction of autophagic pathway (summarized in Fig. 7). Since nutrients are known to modulate autophagic pathway (Hotamisligil, 2017; Hotamisligil and Erbay, 2008), our results highlighted a need to investigate the changes of autophagic pathway following co-exposure to nutrients and NPs, in addition to the changes of colloidal properties of NPs, NP-cell interactions and oxidative stress as suggested before (Cao et al., 2016; McClements et al., 2017). In the future, it is necessary to

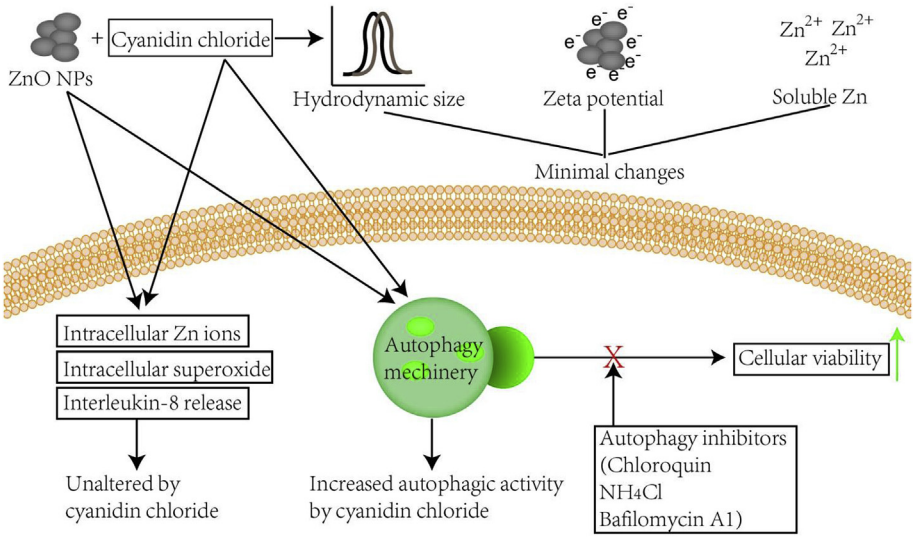

Fig. 7. The proposed influence of CC on ZnO NPs. CC has only minimal impact on hydrodynamic size, Zeta potential and solubility of ZnO NPs. Intracellular superoxide, Zn ions and IL-8 release after ZnO NP exposure are not affected by CC. Rather, CC enhances autophagic activity, which can consequently promote cellular viability after ZnO NP exposure. The presence of autophagic inhibitors abolishes the cytoprotective effects of ZnO NPs. See more in text.

further investigate the influence of anthocyanidins on the toxicity of metal-based NPs. The exact role of induction of autophagy following co-exposure to anthocyanidins and NPs may also need further studies.

Conflicts of interest

No.

Acknowledgement

This work was financially supported by Natural Science Foundation of Hunan Province (Grant No. 2017JJ3348).

Transparency document

Transparency document related to this article can be found online at https://doi.org/10.1016/j.fct.2019.03.047

Appendix A. Supplementary data

Supplementary data related to this article can be found at https://doi.org/10.1016/j.fct.2019.03.047.

References

Abbott Chalew, T.E., Schwab, K.J., 2013. Toxicity of commercially available engineered nanoparticles to Caco-2 and SW480 human intestinal epithelial cells. Cell Biol. Toxicol. 29, 101–116.
Anozie, U.C., Dalhaimer, P., 2017. Molecular links among non-biodegradable nanoparticles, reactive oxygen species, and autophagy. Adv. Drug Deliv. Rev. 122, 65–73.
Belwal, T., Nabavi, S.F., Nabavi, S.M., Habtemariam, S., 2017. Dietary anthocyanins and insulin resistance: when food becomes a medicine. Nutrients 9, E1111.
Cao, Y., Li, J., Liu, F., Li, X., Jiang, Q., Cheng, S., Gu, Y., 2016. Consideration of interaction between nanoparticles and food components for the safety assessment of nanoparticles following oral exposure: a review. Environ. Toxicol. Pharmacol. 46, 206–210.
Cao, Y., Xie, Y., Liu, L., Xiao, A., Li, Y., Zhang, C., Fang, X., Zhou, Y., 2017. Influence of phytochemicals on the biocompatibility of inorganic nanoparticles: a state-of-the-art review. Phytochemistry Rev. 16, 555–563.
Chen, Z., Wang, Y., Zhuo, L., Chen, S., Zhao, L., Chen, T., Li, Y., Zhang, W., Gao, X., Li, P., Wang, H., Jia, G., 2015. Interaction of titanium dioxide nanoparticles with glucose on young rats after oral administration. Nanomedicine 11, 1633–1642.
Choe, Y.J., Ha, T.J., Ko, K.W., Lee, S.Y., Shin, S.J., Kim, H.S., 2012. Anthocyanins in the black soybean (Glycine max L.) protect U2OS cells from apoptosis by inducing autophagy via the activation of adenosyl monophosphate-dependent protein kinase. Oncol. Rep. 28, 2049–2056.
Fang, X., Jiang, L., Gong, Y., Li, J., Liu, L., Cao, Y., 2017. The presence of oleate stabilized ZnO nanoparticles (NPs) and reduced the toxicity of aged NPs to Caco-2 and HepG2 cells. Chem. Biol. Interact. 278, 40–47.
Feng, X., Chen, A., Zhang, Y., Wang, J., Shao, L., Wei, L., 2015. Application of dental nanomaterials: potential toxicity to the central nervous system. Int. J. Nanomed. 10, 3547–3565.
Gaillet, S., Rouanet, J.M., 2015. Silver nanoparticles: their potential toxic effects after oral exposure and underlying mechanisms–a review. Food Chem. Toxicol. 77, 58–63.
Go, M.R., Yu, J., Bae, S.H., Kim, H.J., Choi, S.J., 2018. Effects of interactions between ZnO nanoparticles and saccharides on biological responses. Int. J. Mol. Sci. 19, E486.
Go, M.R., Bae, S.H., Kim, H.J., Yu, J., Choi, S.J., 2017. Interactions between food additive silica nanoparticles and food matrices. Front. Microbiol. 8, 1013.
Gong, Y., Ji, Y., Liu, F., Li, J., Cao, Y., 2017a. Cytotoxicity, oxidative stress and inflammation induced by ZnO nanoparticles in endothelial cells: interaction with palmitate or lipopolysaccharide. J. Appl. Toxicol. 37, 895–901.
Gong, Y., Liu, L., Li, J., Cao, Y., 2017b. The presence of palmitate affected the colloidal stability of ZnO NPs but not the toxicity to Caco-2 cells. J. Nano Res. 19, 335.
Hotamisligil, G.S., 2017. Inflammation, metaflammation and immunometabolic disorders. Nature 542, 177–185.
Hotamisligil, G.S., Erbay, E., 2008. Nutrient sensing and inflammation in metabolic diseases. Nat. Rev. Immunol. 8, 923–934.
Jain, A., Ranjan, S., Dasgupta, N., Ramalingam, C., 2018. Nanomaterials in Food and Agriculture: an overview on their safety concerns and regulatory issues. Crit. Rev. Food Sci. Nutr. 58, 297–317.
Jiang, Q., Li, X., Cheng, S., Gu, Y., Chen, G., Shen, Y., Xie, Y., Cao, Y., 2016. Combined effects of low levels of palmitate on toxicity of ZnO nanoparticles to THP-1 macrophages. Environ. Toxicol. Pharmacol. 48, 103–109.
Khoo, H.E., Azlan, A., Tang, S.T., Lim, S.M., 2017. Anthocyanidins and anthocyanins: colored pigments as food, pharmaceutical ingredients, and the potential health benefits. Food Nutr. Res. 61, 1361779.
Kimura, T., Takabatake, Y., Takahashi, A., Isaka, Y., 2013. Chloroquine in cancer therapy: a double-edged sword of autophagy. Cancer Res. 73, 3–7.
Krol, A., Pomastowski, P., Rafinska, K., Railean-Plugaru, V., Buszewski, B., 2017. Zinc oxide nanoparticles: synthesis, antiseptic activity and toxicity mechanism. Adv. Colloid Interfac. Sci. 249, 37–52.
Laha, D., Pramanik, A., Maity, J., Mukherjee, A., Pramanik, P., Laskar, A., Karmakar, P., 2014. Interplay between autophagy and apoptosis mediated by copper oxide nanoparticles in human breast cancer cells MCF7. Biochim. Biophys. Acta 1840, 1–9.
Lee, J.A., Kim, M.K., Song, J.H., Jo, M.R., Yu, J., Kim, K.M., Kim, Y.R., Oh, J.M., Choi, S.J., 2017. Biokinetics of food additive silica nanoparticles and their interactions with food components. Colloids Surfac. B Biointerfac. 150, 384–392.
Li, D., Wang, P., Luo, Y., Zhao, M., Chen, F., 2017. Health benefits of anthocyanins and molecular mechanisms: update from recent decade. Crit. Rev. Food Sci. Nutr. 57, 1729–1741.
Li, Y., Zhang, C., Liu, L., Gong, Y., Xie, Y., Cao, Y., 2018. The effects of baicalein or baicalin on the colloidal stability of ZnO nanoparticles (NPs) and toxicity of NPs to Caco-2 cells. Toxicol. Mech. Methods 28, 167–176.
Liao, W., Chen, L., Ma, X., Jiao, R., Li, X., Wang, Y., 2016. Protective effects of kaempferol against reactive oxygen species-induced hemolysis and its antiproliferative activity on human cancer cells. Eur. J. Med. Chem. 114, 24–32.
Liao, W., Liu, Z., Zhang, T., Sun, S., Ye, J., Li, Z., Mao, L., Ren, J., 2018. Enhancement of anti-inflammatory properties of nobiletin in macrophages by a nano-emulsion preparation. J. Agric. Food Chem. 66, 91–98.
Lin, J., Huang, Z., Wu, H., Zhou, W., Jin, P., Wei, P., Zhang, Y., Zheng, F., Zhang, J., Xu, J., Hu, Y., Wang, Y., Li, Y., Gu, N., Wen, L., 2014. Inhibition of autophagy enhances the anticancer activity of silver nanoparticles. Autophagy 10, 2006–2020.
Lin, J., Liu, Y., Wu, H., Huang, Z., Ma, J., Guo, C., Gao, F., Jin, P., Wei, P., Zhang, Y., Liu, L., Zhang, R., Qiu, L., Gu, N., Wen, L., 2018. Key role of TFEB nucleus translocation for silver nanoparticle-induced cytoprotective autophagy. Small 14, e1703711.
Liu, J., Feng, X., Wei, L., Chen, L., Song, B., Shao, L., 2016. The toxicology of ion-shedding zinc oxide nanoparticles. Crit. Rev. Toxicol. 46, 348–384.
Liu, T., Liang, H., Liu, L., Gong, Y., Ding, Y., Liao, G., Cao, Y., 2019. Influence of pristine

and hydrophobic ZnO nanoparticles on cytotoxicity and endoplasmic reticulum (ER) stress-autophagy-apoptosis gene expression in A549-macrophage co-culture. Ecotoxicol. Environ. Saf. 167, 188–195.
Luo, Y., Wu, C., Liu, L., Gong, Y., Peng, S., Xie, Y., Cao, Y., 2018. 3-Hydroxyflavone enhances the toxicity of ZnO nanoparticles in vitro. J. Appl. Toxicol. 38, 1206–1214.
Luo, Y.H., Wu, S.B., Wei, Y.H., Chen, Y.C., Tsai, M.H., Ho, C.C., Lin, S.Y., Yang, C.S., Lin, P., 2013. Cadmium-based quantum dot induced autophagy formation for cell survival via oxidative stress. Chem. Res. Toxicol. 26, 662–673.
Mao, X., Nguyen, T.H., Lin, M., Mustapha, A., 2016. Engineered nanoparticles as potential food contaminants and their toxicity to caco-2 cells. J. Food Sci. 81, T2107–T2113.
Martirosyan, A., Bazes, A., Schneider, Y.J., 2014. In vitro toxicity assessment of silver nanoparticles in the presence of phenolic compounds–preventive agents against the harmful effect? Nanotoxicology 8, 573–582.
Martirosyan, A., Grintzalis, K., Polet, M., Laloux, L., Schneider, Y.J., 2016. Tuning the inflammatory response to silver nanoparticles via quercetin in Caco-2 (co-)cultures as model of the human intestinal mucosa. Toxicol. Lett. 253, 36–45.
McClements, D.J., Xiao, H., Demokritou, P., 2017. Physicochemical and colloidal aspects of food matrix effects on gastrointestinal fate of ingested inorganic nanoparticles. Adv. Colloid Interface Sci. 246, 165–180.
McCracken, C., Dutta, P.K., Waldman, W.J., 2016. Critical assessment of toxicological effects of ingested nanoparticles. Environ. Sci.: Nano 3, 256–282.
Moore, T.L., Rodriguez-Lorenzo, L., Hirsch, V., Balog, S., Urban, D., Jud, C., Rothen-Rutishauser, B., Lattuada, M., Petri-Fink, A., 2015. Nanoparticle colloidal stability in cell culture media and impact on cellular interactions. Chem. Soc. Rev. 44, 6287–6305.
Moosavi, M.A., Haghi, A., Rahmati, M., Taniguchi, H., Mocan, A., Echeverria, J., Gupta, V.K., Tzvetkov, N.T., Atanasov, A.G., 2018. Phytochemicals as potent modulators of autophagy for cancer therapy. Cancer Lett. 424, 46–69.
Moreno-Olivas, F., Tako, E., Mahler, G.J., 2019. ZnO nanoparticles affect nutrient transport in an in vitro model of the small intestine. Food Chem. Toxicol. 124, 112–127.
Ongkowijoyo, P., Luna-Vital, D.A., Gonzalez de, M.E., 2018. Extraction techniques and analysis of anthocyanins from food sources by mass spectrometry: an update. Food Chem. 250, 113–126.
Pathakoti, K., Manubolu, M., Hwang, H.M., 2017. Nanostructures: current uses and future applications in food science. J. Food Drug Anal. 25, 245–253.
Pesonen, M., Vahakangas, K., 2019. Autophagy in exposure to environmental chemicals. Toxicol. Lett. 305, 1–9.
Qian, P., Yan, L.J., Li, Y.Q., Yang, H.T., Duan, H.Y., Wu, J.T., Fan, X.W., Wang, S.L., 2018. Cyanidin ameliorates cisplatin-induced cardiotoxicity via inhibition of ROS-mediated apoptosis. Exp. Ther. Med. 15, 1959–1965.
Saptarshi, S.R., Duschl, A., Lopata, A.L., 2015. Biological reactivity of zinc oxide nanoparticles with mammalian test systems: an overview. Nanomedicine. (Lond). 10, 2075–2092.
Song, Y., Guan, R., Lyu, F., Kang, T., Wu, Y., Chen, X., 2014. In vitro cytotoxicity of silver nanoparticles and zinc oxide nanoparticles to human epithelial colorectal adenocarcinoma (Caco-2) cells. Mutat. Res. 769, 113–118.
Tsapras, P., Nezis, I.P., 2017. Caspase involvement in autophagy. Cell Death Differ. 24, 1369–1379.
Vance, M.E., Kuiken, T., Vejerano, E.P., McGinnis, S.P., Hochella Jr., M.F., Rejeski, D., Hull, M.S., 2015. Nanotechnology in the real world: redeveloping the nanomaterial consumer products inventory. Beilstein J. Nanotechnol. 6, 1769–1780.
Wang, H., Du, L.J., Song, Z.M., Chen, X.X., 2013. Progress in the characterization and safety evaluation of engineered inorganic nanomaterials in food. Nanomedicine. (Lond). 8, 2007–2025.
Wang, H., Lu, Z., Wang, L., Guo, T., Wu, J., Wan, J., Zhou, L., Li, H., Li, Z., Jiang, D., Song, P., Xie, H., Zhou, L., Xu, X., Zheng, S., 2017a. New generation nanomedicines constructed from self-assembling small-molecule prodrugs alleviate cancer drug toxicity. Cancer Res. 77, 6963–6974.
Wang, L., Hu, C., Shao, L., 2017b. The antimicrobial activity of nanoparticles: present situation and prospects for the future. Int. J. Nanomed. 12, 1227–1249.
Wang, L., Yun, L., Wang, X., Sha, L., Wang, L., Sui, Y., Zhang, H., 2019. Endoplasmic reticulum stress triggered by Soyasapogenol B promotes apoptosis and autophagy in colorectal cancer. Life Sci. 218, 16–24.
Wang, Y., Yuan, L., Yao, C., Ding, L., Li, C., Fang, J., Sui, K., Liu, Y., Wu, M., 2014. A combined toxicity study of zinc oxide nanoparticles and vitamin C in food additives. Nanoscale 6, 15333–15342.
Wen, L., Jiang, X., Sun, J., Li, X., Li, X., Tian, L., Li, Y., Bai, W., 2018. Cyanidin-3-O-glucoside promotes the biosynthesis of progesterone through the protection of mitochondrial function in Pb-exposed rat leydig cells. Food Chem. Toxicol. 112, 427–434.
Xia, C.Y., Zhang, S., Chu, S.F., Wang, Z.Z., Song, X.Y., Zuo, W., Gao, Y., Yang, P.F., Chen, N.H., 2016. Autophagic flux regulates microglial phenotype according to the time of oxygen-glucose deprivation/reperfusion. Int. Immunopharmacol. 39, 140–148.
Xiang, S., Yang, P., Guo, H., Zhang, S., Zhang, X., Zhu, F., Li, Y., 2017. Green tea makes polyphenol nanoparticles with radical-scavenging activities. Macromol. Rapid Commun. 38, 10.
Yang, Y., Wang, X., Liao, G., Liu, X., Chen, Q., Li, H., Lu, L., Zhao, P., Yu, Z., 2018. iRGD-decorated red shift emissive carbon nanodots for tumor targeting fluorescence imaging. J. Colloid Interface Sci. 509, 515–521.
Zhang, C., Li, Y., Liu, L., Gong, Y., Xie, Y., Cao, Y., 2018. Chemical structures of polyphenols that critically influence the toxicity of ZnO nanoparticles. J. Agric. Food Chem. 66, 1714–1722.